

Theory of diode effect in d -wave superconductor junctions on the surface of topological insulator

Yukio Tanaka¹, Bo Lu², and Naoto Nagaosa^{3,4}

¹*Department of Applied Physics, Nagoya University, Nagoya, 464-8603, Japan*

²*Center for Joint Quantum Studies and Department of Physics,
Tianjin University, Tianjin 300072, China*

³*Center for Emergent Matter Science (CEMS),
RIKEN, Wako, Saitama 351-0198, Japan*

⁴*Department of Applied Physics, The University of Tokyo, Tokyo 113-8656, Japan*

(Dated: May 27, 2022)

Abstract

We study theoretically the Josephson junction S/FI/S (S: d-wave superconductor, FI: ferromagnetic insulator) on the surface of a topological insulator. We find it can show a very large nonreciprocity, i.e., diode effect, by tuning the crystal axis of *d*-wave superconductor and the magnetization in FI. The difference of the upper critical currents I_c 's between the positive (I_c^+) and negative (I_c^-) directions can be about factor 2, where the current-phase relation can be modified largely from the conventional one, due to the simultaneous presence of $\sin(\varphi)$, $\sin(2\varphi)$ and $\cos(\varphi)$ components with φ being the macroscopic phase difference between two superconductors. The predicted quality factor Q characterizing the diode effect has a strong temperature dependence and its sign is reversed by the change of the direction of the magnetization in FI. The enhancement of Q at low temperature stems from the Majorana bound states at the interface. This result can pave a way to realize an efficient superconducting diode with low energy cost.

I. INTRODUCTION

Nonreciprocal responses of quantum matters attract recent intensive interests [1]. With broken inversion symmetry \mathcal{P} , it is generally expected that the response to the external field is different from that of the field in the opposite direction. When the flow of electrons, i.e., current, is concerned, the reversal of the arrow of time, i.e., the time-reversal symmetry \mathcal{T} is also relevant, and it often happens that the nonreciprocal transport occurs when both \mathcal{P} and \mathcal{T} are broken simultaneously although only \mathcal{P} breaking is enough in some cases. In the normal state of the conductor, the typical energy scale is the Fermi energy of the order of eV, which is large compared with the spin-orbit interaction and Zeeman energy due to external magnetic field, both of which are needed to introduce the asymmetry of the energy band dispersion $\varepsilon_n(k)$ between k and $-k$. Therefore, the value of γ , which characterizes the strength of the nonreciprocal resistivity in the empirical expression

$$\rho(I) = \rho_0(1 + \gamma IB), \quad (\text{I.1})$$

is usually very small typically of the order of $\sim 10^{-3} - 10^{-1} \text{A}^{-1} \text{T}^{-1}$ [2–5]. Here ρ_0 is the linear resistivity without magnetic field, I is the current, and B is the magnetic field. This phenomenon is called magneto-chiral anisotropy (MCA). It has been reported that γ reaches of the order of $1 \text{A}^{-1} \text{T}^{-1}$ in BiTeBr, which shows a gigantic bulk Rashba splitting [6].

MCA can occur also in superconductors, where the resistivity is finite above the transition temperature or due to the vortices [7]. Especially, the noncentrosymmetric two-dimensional superconductors have been studied from this viewpoint, and the very large γ -values $\sim 10^3 - 10^4 \text{A}^{-1} \text{T}^{-1}$ compared with the normal state are realized there [8]. It is interpreted as the replacement of the energy denominator from the Fermi energy to the superconducting gap energy, corresponding to the difference between the fermionic and bosonic transport. Some other superconductors are reported to show MCA [9, 10].

The nonreciprocal response can be also defined without the resistivity expressed in eq.(I.1). Instead, the critical current I_c can depend on the direction of the current. In ref.[11], this nonreciprocal I_c was observed in an artificial superlattice $[\text{Nb/V/Ta}]_n$ under an external magnetic field. The difference $\Delta I_c = I_c^+ - |I_c^-|$ is typically 0.2mA while $I_c^+ (|I_c^-|) \cong 6\text{mA}$, which indicates that the magnitude of the nonreciprocity is of the order of a few %. Theories of nonreciprocal critical current, i.e., ΔI_c , have been developed recently [12–17]. Note also that a recent experiment found the Josephson diode effect even without the external magnetic field [18].

Compared with this bulk transport in superconductors, the Josephson junction might show the much larger diode effect, because the kinetic energy at the junction is suppressed and the interaction effect can be enhanced. In addition, the Andreev bound states at the interface can play some role in the diode effect. In [19], the asymmetric charging energy, which acts as the "kinetic energy" of the Josephson phase φ , leads to the diode effect through the nonreciprocal dynamics of φ . In this scenario, no time-reversal symmetry breaking is needed. On the other hand, with \mathcal{T} breaking, the nonreciprocal current-phase relation can lead to the diode effect even without the charging energy, which we pursue in the present paper. Our target system is the superconductor (S) / Ferromagnet(F) /S junction on a three-dimensional topological insulator (TI) where pairing symmetry of superconductor is d -wave.

It is known that the standard current-phase relation (CPR) of Josephson current $I(\varphi)$ between two superconductors is $I(\varphi) \sim \sin \varphi$, where the φ is the macroscopic phase difference between two superconductors. However, if we consider unconventional superconductors like d -wave one, a wide variety of current phase relations appears. For d -wave superconductor junctions, when the lobe direction of d -wave pair potential and the normal to the interface is not parallel, so called Andreev bound state (ABS) is generated at the interface due to

the sign change of the d -wave pair potential on the Fermi surface [20–23]. The presence of ABS enhances the $\sin 2\varphi$ component of $I(\varphi)$ and the resulting free energy minimum of the junction can locate neither at $\varphi = 0$ nor $\pm\pi$ [24, 25]. Also, the non-monotonic temperature dependence of Josephson current is generated by ABS depending on the direction of the crystal axis of d -wave pair potential [25–28].

If we put $S/FI/S$ junction with d -wave superconductors on the surface of TI, ABS becomes Majorana fermion due to the spin-momentum locking specific to TI [29, 30]. This system breaks both \mathcal{P} and \mathcal{T} symmetry and an exotic current-phase relation with $I(\varphi) \neq -I(-\varphi)$ has been actually predicted [31]. Although the previous article has not reported the nonreciprocity of Josephson current [31], we anticipate that the positive maximum magnitude of $I(\varphi)$ I_c^+ and the negative one I_c^- can take the different value each other by searching various configurations of the junctions.

In this paper, we calculate Josephson current in d -wave superconductor ($x < 0$)/ferromagnet ($0 < x < d$)/ d -wave superconductor ($x > d$)(DS/FI/DS) junction on a 3D topological insulator (TI) surface. We choose the ferromagnetic insulator (FI) as a ferromagnet to generate Majorana bound state between DS/FI interface. We show anomalous current phase relation and the energy dispersion of the Majorana bound state. A giant diode effect with a huge quality factor Q is obtained by tuning the crystal axis of d -wave superconductor. We also clarify the strong temperature dependence of Q due to the presence of low energy Majorana bound state. It is revealed how the sign of Q is controlled by the direction of magnetization.

The organization of this paper is as follows. We explain the model and formulation in section II. The detailed expressions of the Andreev reflection coefficients are shown since these quantities are essential to understand the current-phase relation $I(\varphi)$ for various parameters. Section III shows numerically obtained results about $I(\varphi)$, Q and dispersion of Majorana bound states. In section IV, we conclude our results.

II. MODEL AND FORMULATION

We consider a d -wave superconductor ($x < 0$)/ferromagnetic insulator ($0 < x < d$)/ d -wave superconductor ($x > d$)(DS/FI/DS) junction on a 3D topological insulator (TI) surface as depicted in Fig.1. The effective Hamiltonian for the BdG equations is given by

[31]

$$\mathcal{H} = \begin{bmatrix} \hat{h}(k_x, k_y) + \hat{M} & i\hat{\sigma}_y \Delta(\theta, x) \\ -i\hat{\sigma}_y \Delta^*(\theta, x) & -\hat{h}^*(-k_x, -k_y) - \hat{M}^* \end{bmatrix}, \quad (\text{II.1})$$

with

$$\hat{h}(k_x, k_y) = v_f(k_x \hat{\sigma}_x + k_y \hat{\sigma}_y) - \mu[\Theta(-x) + \Theta(x-d)], \quad k_x = \frac{\partial}{i\partial x}, \quad k_y = \frac{\partial}{i\partial y}$$

where $\hat{\sigma}_{x,y,z}$ is the Pauli matrix in the spin space with $\hbar = 1$ unit. μ is the chemical potential in the superconducting region with $\mu = vk_F$ and $x(y)$ component of the Fermi momentum k_F is given by $(k_{Fx}, k_{Fy}) = k_F(\cos\theta, \sin\theta)$ with an injection angle θ . Chemical potential in FI is set to be zero and the exchange field in FI region is given by [32]

$$\hat{M} = m_z \hat{\sigma}_z \Theta(x) \Theta(L-x)$$

and the pair potential of d -wave superconductor is expressed by [25]

$$\Delta(\theta, x) = \begin{cases} \Delta_{L\pm}(\theta) = \Delta_0 \cos[2(\theta \mp \alpha)] \exp(i\varphi), & x < 0 \\ \Delta_{R\pm}(\theta) = \Delta_0 \cos[2(\theta \mp \beta)], & x > d, \end{cases} \quad (\text{II.2})$$

Here, α and β denote angles between the x -axis and the lobe direction of the pair potential of d -wave superconductor as shown in Fig. 1.

BdG wave function of the above Hamiltonian is given by

$$\Psi(\mathbf{x}) = \exp(ik_y y) [\Psi_{SL}(x) \Theta(-x) + \Psi_{FI}(x) \Theta(x) \Theta(d-x) + \Psi_{SR}(x) \Theta(x-d)]$$

with the momentum parallel to the interface $k_y = k_F \sin\theta$. We denote the quasiparticle energy measured from the Fermi surface as E and assume the condition where $|E| \ll \mu$, $\Delta_0 \ll \mu$, $|E| \ll |m_z|$, and $\Delta_0 \ll |m_z|$ are satisfied. If we consider an electron-like quasiparticle injection from the left superconductor, $\Psi_{SL}(x)$, $\Psi_{FI}(x)$, $\Psi_{SR}(x)$ are given by

$$\Psi_{SL}(x) = (\Psi_{in}^e + a_e \Psi_{hr}) \exp(ik_x x) + b_e \Psi_{er} \exp(-ik_x x) \quad (\text{II.3})$$

$$\begin{aligned} \Psi_{FI}(x) = & f_{1e} \Psi_{e1} \exp(-\kappa_{ex} x) + f_{2e} \Psi_{e2} \exp(\kappa_{ex} x) \\ & + f_{3e} \Psi_{h1} \exp(\kappa_{hx} x) + f_{4e} \Psi_{h2} \exp(-\kappa_{hx} x) \end{aligned} \quad (\text{II.4})$$

$$\Psi_{SR}(x) = c_e \Psi_{et} \exp(ik_x x) + d_e \Psi_{ht} \exp(-ik_x x) \quad (\text{II.5})$$

$$k_x = \sqrt{(\mu/v)^2 - k_y^2}, \quad \kappa_{ex} = \kappa_{hx} = \sqrt{m_z^2 + v^2 k_y^2}/v.$$

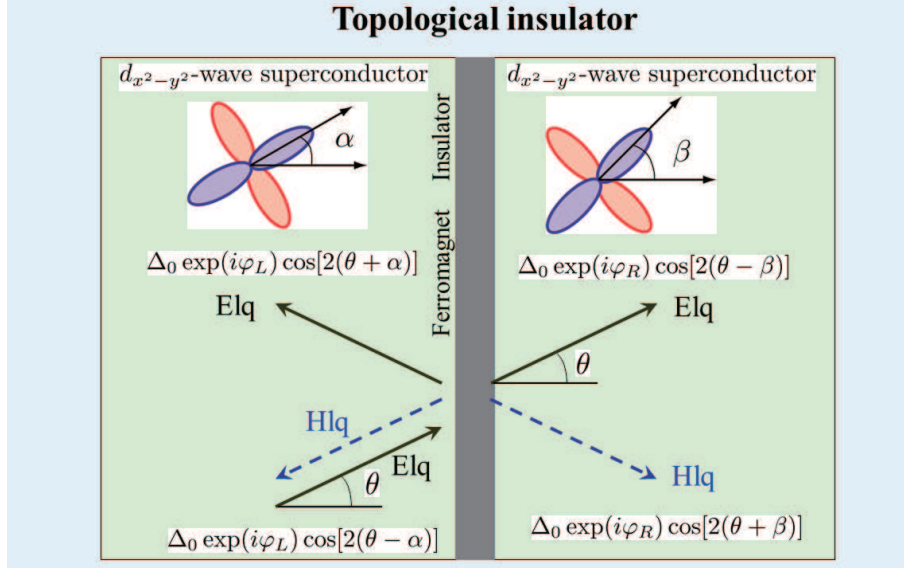


FIG. 1. Schematic illustration of the d -wave superconductor junctions on the surface of topological insulator (TI). An electron-like quasiparticle (Elq) is injected and it is reflected or transmitted as Elq and hole-like quasiparticle (Hlq).

Ψ_{in}^e , Ψ_{hr} , Ψ_{er} defined in the left superconductor are given by

$$\Psi_{in}^e = \begin{pmatrix} 1 \\ \exp(i\theta) \\ -\Gamma_{L+} \exp[i(\theta - \varphi)] \\ \Gamma_{L+} \exp(-i\varphi) \end{pmatrix}, \quad \Psi_{hr} = \begin{pmatrix} \Gamma_{L+} \\ \Gamma_{L+} \exp(i\theta) \\ -\exp[i(\theta - \varphi)] \\ \exp(-i\varphi) \end{pmatrix}, \quad \Psi_{er} = \begin{pmatrix} 1 \\ -\exp(-i\theta) \\ \Gamma_{L-} \exp[-i(\theta + \varphi)] \\ \Gamma_{L-} \exp(-i\varphi) \end{pmatrix} \quad (\text{II.6})$$

with $\exp(i\theta) = (k_x + ik_y)/k_F$. Ψ_{e1} , Ψ_{e2} , Ψ_{h1} , and Ψ_{h2} in FI are

$$\Psi_{e1} = \begin{pmatrix} i\gamma \\ 1 \\ 0 \\ 0 \end{pmatrix}, \quad \Psi_{e2} = \begin{pmatrix} -i\gamma^{-1} \\ 1 \\ 0 \\ 0 \end{pmatrix}, \quad \Psi_{h1} = \begin{pmatrix} 0 \\ 0 \\ i\gamma \\ 1 \end{pmatrix}, \quad \Psi_{h2} = \begin{pmatrix} 0 \\ 0 \\ -i\gamma^{-1} \\ 1 \end{pmatrix} \quad (\text{II.7})$$

$\gamma = -v(\kappa_{ex} - k_y)/m_z$. Ψ_{et} , Ψ_{ht} in the right superconductor are given by

$$\Psi_{et} = \begin{pmatrix} 1 \\ \exp(i\theta) \\ -\Gamma_{R+} \exp(i\theta) \\ \Gamma_{R+} \end{pmatrix}, \quad \Psi_{ht} = \begin{pmatrix} \Gamma_{R-} \\ -\Gamma_{R-} \exp(-i\theta) \\ \exp(-i\theta) \\ 1 \end{pmatrix} \quad (\text{II.8})$$

with

$$\Gamma_{L\pm} = \frac{\Delta_{L\pm}(\theta)}{E + \sqrt{E^2 - \Delta_{L\pm}^2}}, \quad \Gamma_{R\pm} = \frac{\Delta_{R\pm}(\theta)}{E + \sqrt{E^2 - \Delta_{R\pm}^2}}.$$

We can also calculate the wave function corresponding to eqs. (II.3), (II.4), and (II.5) with hole-like quasiparticle injection as follows.

$$\Psi_{SL}(x) = (\Psi_{in}^h + a_h \Psi_{er}) \exp(-ik_x x) + b_e \Psi_{hr} \exp(ik_x x) \quad (\text{II.9})$$

$$\begin{aligned} \Psi_{FI}(x) = & f_{1h} \Psi_{e1} \exp(-\kappa_{ex} x) + f_{2h} \Psi_{e2} \exp(\kappa_{ex} x) \\ & + f_{3h} \Psi_{h1} \exp(\kappa_{hx} x) + f_{4h} \Psi_{h2} \exp(-\kappa_{hx} x) \end{aligned} \quad (\text{II.10})$$

$$\Psi_{SR}(x) = c_h \Psi_{et} \exp(ik_x x) + d_h \Psi_{ht} \exp(-ik_x x) \quad (\text{II.11})$$

with

$$\Psi_{in}^h = \begin{pmatrix} \Gamma_{L-} \\ -\Gamma_{L-} \exp(-i\theta) \\ \exp[-i(\theta + \varphi)] \\ \exp(-i\varphi) \end{pmatrix}.$$

$\Psi_{SL}(x)$, $\Psi_{FI}(x)$ and $\Psi_{SR}(x)$ satisfy the boundary condition $\Psi_{SL}(x=0) = \Psi_{FI}(x=0)$ and $\Psi_{FI}(x=d) = \Psi_{SR}(x=d)$. The Andreev reflection coefficients a_e and a_h are needed to calculate Josephson current [25, 33]. They are given by

$$a_e = -\frac{\sigma_N \Lambda_{1e} + (1 - \sigma_N) \Lambda_{2e}}{\Lambda_d(E, \theta)}, \quad a_h = -\frac{\sigma_N \Lambda_{1h} + (1 - \sigma_N) \Lambda_{2h}}{\Lambda_d(E, \theta)} \quad (\text{II.12})$$

with

$$\begin{aligned} \Lambda_d(E, \theta) = & [1 - \sigma_N] [1 + \exp(-i\eta) \Gamma_{R+} \Gamma_{R-}] [1 + \exp(i\eta) \Gamma_{L+} \Gamma_{L-}] \\ & + \sigma_N [1 - \exp(-i\varphi) \Gamma_{L-} \Gamma_{R-}] [1 - \exp(i\varphi) \Gamma_{L+} \Gamma_{R+}] \end{aligned} \quad (\text{II.13})$$

$$\begin{aligned} \Lambda_{1e} = & [1 - \exp(-i\varphi) \Gamma_{L-} \Gamma_{R-}] [\Gamma_{L+} - \Gamma_{R+} \exp(i\varphi)] \\ \Lambda_{2e} = & [1 + \exp(-i\eta) \Gamma_{R+} \Gamma_{R-}] [\Gamma_{L+} + \exp(i\eta) \Gamma_{L-}] \end{aligned} \quad (\text{II.14})$$

$$\begin{aligned} \Lambda_{1h} = & [1 - \exp(i\varphi) \Gamma_{L+} \Gamma_{R+}] [\Gamma_{L-} - \Gamma_{R-} \exp(-i\varphi)] \\ \Lambda_{2e} = & [1 + \exp(-i\eta) \Gamma_{R+} \Gamma_{R-}] [\Gamma_{L-} + \exp(i\eta) \Gamma_{L+}] \end{aligned} \quad (\text{II.15})$$

and

$$\exp(i\eta) = \cos \eta + i \sin \eta$$

$$\cos \eta = \frac{m_z^2 \cos^2 \theta - \mu^2 \sin^2 \theta}{m_z^2 \cos^2 \theta + \mu^2 \sin^2 \theta}, \quad \sin \eta = \frac{-2m_z \mu \cos \theta \sin \theta}{m_z^2 \cos^2 \theta + \mu^2 \sin^2 \theta}.$$

Here, σ_N is the transparency at this junction in the normal state and it is given by

$$\sigma_N = \frac{\cos^2 \theta}{\cosh^2(\kappa_{ex}d) \cos^2 \theta + \sinh^2(\kappa_{ex}d) \sin^2 \theta \sin^2(\frac{\eta}{2})} \quad (\text{II.16})$$

Based on the Green's function of BdG equation, it is known that Josephson current is expressed by a_{en} and a_{hn} which are obtained from the analytical continuation from E to $i\omega_n$ in a_e and a_h [33] where $\omega_n = 2\pi k_B T(n + 1/2)$ is the Matsubara frequency. The resulting Josephson current $I(\varphi)$ is given by [25, 31]

$$R_N I(\varphi) = \frac{\pi \bar{R}_N k_B T}{e} \left\{ \sum_{\omega_n} \int_{-\pi/2}^{\pi/2} \left[\frac{a_{en}(\theta, \varphi)}{\Omega_{nL+}} \Delta_{L+}(\theta) - \frac{a_{hn}(\theta, \varphi)}{\Omega_{L-}} \Delta_{L-}(\theta) \right] \cos \theta d\theta \right\} \quad (\text{II.17})$$

with

$$\bar{R}_N^{-1} = \int_{-\pi/2}^{\pi/2} \sigma_N \cos \theta d\theta, \quad \Omega_{nL\pm} = \text{sgn}(\omega_n) \sqrt{\Delta_L^2(\theta_{\pm}) + \omega_n^2}$$

and

$$a_{en} = i \frac{\sigma_N \Lambda_{1en} + (1 - \sigma_N) \Lambda_{2en}}{\Lambda_{dn}(\theta)}, \quad a_{hn} = i \frac{\sigma_N \Lambda_{1hn} + (1 - \sigma_N) \Lambda_{2hn}}{\Lambda_{dn}(\theta)} \quad (\text{II.18})$$

with

$$\Lambda_{dn}(\theta) = [1 - \sigma_N] [1 - \exp(-i\eta) \Gamma_{nR+} \Gamma_{nR-}] [1 - \exp(i\eta) \Gamma_{nL+} \Gamma_{nL-}]$$

$$+ \sigma_N [1 + \exp(-i\varphi) \Gamma_{L-} \Gamma_{R-}] [1 + \exp(i\varphi) \Gamma_{L+} \Gamma_{R+}] \quad (\text{II.19})$$

$$\Lambda_{1en} = [1 + \exp(-i\varphi) \Gamma_{nL-} \Gamma_{nR-}] [\Gamma_{nL+} - \Gamma_{nR+} \exp(i\varphi)]$$

$$\Lambda_{2en} = [1 - \exp(-i\eta) \Gamma_{nR+} \Gamma_{nR-}] [\Gamma_{nL+} + \exp(i\eta) \Gamma_{nL-}] \quad (\text{II.20})$$

$$\Lambda_{1hn} = [1 + \exp(i\varphi) \Gamma_{nL+} \Gamma_{nR+}] [\Gamma_{nL-} - \Gamma_{nR-} \exp(-i\varphi)]$$

$$\Lambda_{2en} = [1 - \exp(-i\eta) \Gamma_{nR+} \Gamma_{nR-}] [\Gamma_{nL-} + \exp(i\eta) \Gamma_{nL+}] \quad (\text{II.21})$$

with

$$\Gamma_{nL\pm} = \frac{\Delta_{L\pm}(\theta)}{\omega_n + \Omega_{nL\pm}}, \quad \Gamma_{nR\pm} = \frac{\Delta_{R\pm}(\theta)}{\omega_n + \Omega_{nR\pm}}$$

By using $\Gamma_{nL\pm}(\theta) = \Gamma_{nL\mp}(-\theta)$, $\Gamma_{nR\pm}(\theta) = \Gamma_{nR\mp}(-\theta)$,

$$R_N I(\varphi) = \frac{\pi \bar{R}_N k_B T}{e} \sum_n \int_{-\pi/2}^{\pi/2} d\theta \frac{4\Gamma_{nL+}\Gamma_{nR+}}{|\Lambda_{dn}(\theta)|^2} \cos \theta \sigma_N F(\theta, i\omega_n, \varphi) \quad (\text{II.22})$$

$$F(\theta, i\omega_n, \varphi) = (1 - \sigma_N) \Lambda_{1n} + \sigma_N \sin \varphi |1 + \exp(i\varphi) \Gamma_{nL-} \Gamma_{nR-}|^2 \quad (\text{II.23})$$

with

$$\begin{aligned} \Lambda_{1n} = & \sin \varphi \text{Real} [(1 - \exp(i\eta) \Gamma_{nL+} \Gamma_{nL-}) (1 - \exp(-i\eta) \Gamma_{nR+} \Gamma_{nR-})] \\ & + \cos \varphi \sin \eta (\Gamma_{nL+} \Gamma_{nL-} - \Gamma_{nR+} \Gamma_{nR-}). \end{aligned} \quad (\text{II.24})$$

The obtained $I(\varphi)$ reproduces standard formula of d -wave superconductor junctions without TI [25–27, 34] by choosing $\eta = \pi$. In the next section, by using eqs. (II.22) and (II.23), we calculate $I(\varphi)$ and quality factor Q . In order to prove the m_z , α , and β dependence of $I(\varphi)$ analytically, it is convenient to transform $F(\theta, i\omega_n, \varphi)$ in eqs. (II.22) and (II.23) as follows.

$$F(\theta, i\omega_n, \varphi) = (1 - \sigma_N) (\sin \varphi \Lambda_{ne} + \cos \varphi \Lambda_{no}) + \sigma_N [\sin \varphi (1 + \Gamma_{nL-}^2 \Gamma_{nR-}^2) + \Gamma_{nL-} \Gamma_{nR-} \sin 2\varphi] \quad (\text{II.25})$$

with

$$\Lambda_{ne} = 1 + \Gamma_{nL+} \Gamma_{nL-} \Gamma_{nR+} \Gamma_{nR-} - \cos \eta (\Gamma_{nL+} \Gamma_{nL-} + \Gamma_{nR+} \Gamma_{nR-}), \quad (\text{II.26})$$

and

$$\Lambda_{no} = (\Gamma_{nL+} \Gamma_{nL-} - \Gamma_{nR+} \Gamma_{nR-}) \sin \eta. \quad (\text{II.27})$$

Here, Λ_{ne} and Λ_{no} are even and odd function of θ , respectively.

III. RESULTS

First, let us focus on the current phase relation. As shown later, the quality factor Q depends sensitively on the angles α and β . We pick up the particular value of $\alpha = -0.2\pi$ and 0.09π , where Q is hugely enhanced, and examine the current-phase relation (CPR). At this value of α, β , we obtain quite exotic CPR shown in Fig. 2A.

As seen from curves (a) and (b) of Fig. 2, the magnitude of I_c^+ and I_c^- are different from each other, where I_c^+ (I_c^-) is the positive (negative) maximum value of $I(\varphi)$. Since the quality factor showing nonreciprocity is expressed by

$$Q = \frac{I_c^+ - |I_c^-|}{I_c^+ + |I_c^-|} \quad (\text{III.1})$$

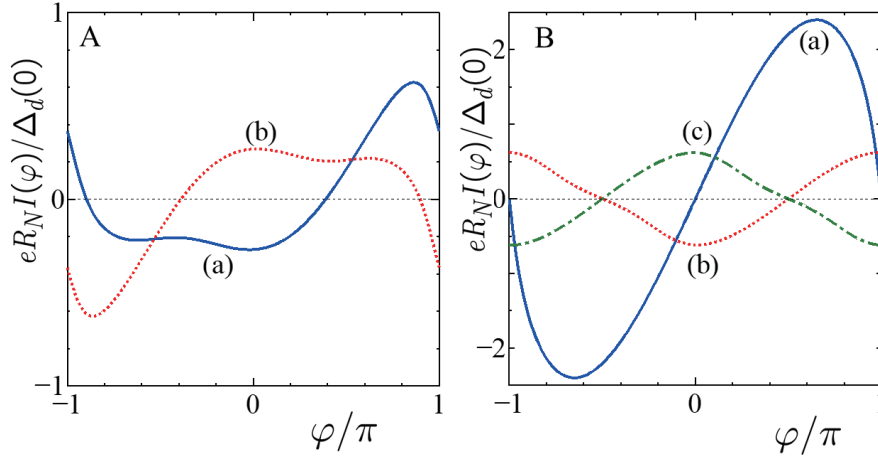


FIG. 2. Current phase relation $I(\varphi)$ is plotted for $T = 0.05T_d$ and $d |m_z| / v = 1$. R_N , $\Delta_d(0)$ and T_d is the resistance of the junction in the normal state, the amplitude of pair potential at zero temperature, and the transition temperature of d -wave superconductor, respectively. A: $\alpha = -0.2\pi$ and $\beta = 0.09\pi$. (a) $m_z = 0.5\mu$, (b) $m_z = -0.5\mu$. B: (a) $\alpha = 0$, $\beta = 0$, (b) $\alpha = 0$, $\beta = 0.25\pi$ and $m_z = 0.5\mu$. (c) $\alpha = 0$, $\beta = 0.25\pi$ and $m_z = -0.5\mu$.

we can expect diode effect. On the other hand, for $\alpha = 0$, $\beta = 0$ (curve (a) in Fig. 2B) $I(\varphi)$ shows a standard sinusoidal behaviour. For $\alpha = 0$, $\beta = \pi/4$, although $I(\varphi)$ shows an unconventional current phase relation with nonzero $I(\varphi)$ at $\varphi = 0$, $I_c^+ = I_c^-$ is still satisfied. By changing the sign of the magnetization from m_z to $-m_z$, $I(\varphi) = I(\varphi, m_z)$ satisfies

$$I(\varphi, m_z) = -I(-\varphi, -m_z) \quad (\text{III.2})$$

as seen from curves (a) and (b) in Fig. 2A and curves (b) and (c) in Fig. 2B. We can show this relation analytically from eqs. (II.22) and (II.25). Since $|\Lambda_{dn}(\theta)|^2 = |\Lambda_{dn}(-\theta)|^2$ is satisfied $I(\varphi)$ is expressed as

$$R_N I(\varphi) = \frac{\pi \bar{R}_N k_B T}{e} \sum_n \int_{-\pi/2}^{\pi/2} d\theta \frac{2 \cos \theta \sigma_N}{|\Lambda_{dn}(\theta)|^2} [A(\theta) \sin \varphi + B(\theta) \sin 2\varphi + C(\theta) \cos \varphi] \quad (\text{III.3})$$

with

$$A(\theta) = (\Gamma_{nL+} \Gamma_{nR+} + \Gamma_{nL-} \Gamma_{nR-}) [(1 - \sigma_N) \Lambda_{ne} + \sigma_N (1 + \Gamma_{nL+} \Gamma_{nL-} \Gamma_{nR+} \Gamma_{nR-})] \quad (\text{III.4})$$

$$B(\theta) = 2\sigma_N \Gamma_{nL+} \Gamma_{nL-} \Gamma_{nR+} \Gamma_{nR-}, \quad C(\theta) = (1 - \sigma_N) (\Gamma_{nL+} \Gamma_{nR+} + \Gamma_{nL-} \Gamma_{nR-}) \Lambda_{no} \quad (\text{III.5})$$

using the definition of Λ_{dn} , Λ_{ne} , and Λ_{no} . Here $A(\theta) = A(-\theta)$, $B(\theta) = B(-\theta)$, and $C(\theta) = C(-\theta)$ are satisfied. Since $\exp(-i\eta)$ changes into $\exp(i\eta)$ by the transformation of θ to $-\theta$ or m_z to $-m_z$, $\Lambda_{dn}(\theta) = \Lambda_{dn}(\theta, m_z, \varphi)$ satisfies

$$\Lambda_{dn}(\theta, -m_z, \varphi) = \Lambda_{dn}(-\theta, m_z, -\varphi), \quad \Lambda_{dn}(-\theta, m_z, \varphi) = \Lambda_{dn}^*(\theta, m_z, \varphi)$$

and

$$|\Lambda_{dn}(\theta, -m_z, \varphi)|^2 = |\Lambda_{dn}(\theta, m_z, -\varphi)|^2 \quad (\text{III.6})$$

Also, $\Lambda_{ne} = \Lambda_{ne}(\theta, m_z)$ and $\Lambda_{no} = \Lambda_{no}(\theta, m_z)$ satisfy

$$\Lambda_{ne}(\theta, m_z) = \Lambda_{ne}(\theta, -m_z), \quad \Lambda_{no}(\theta, m_z) = -\Lambda_{no}(\theta, -m_z).$$

Then, $A(\theta) = A(\theta, m_z)$ and $C(\theta) = C(\theta, m_z)$ satisfies

$$A(\theta, m_z) = A(\theta, -m_z), \quad C(\theta, m_z) = -C(\theta, -m_z)$$

As a result, we can derive eq. (III.2).

From this equation, we can derive qualitative feature of $I(\varphi)$ for typical configurations. For $\alpha = \beta = 0$ ($\alpha = \beta = \pi/4$), owing to $\Gamma_{nL+} = \Gamma_{nL-}$ ($\Gamma_{nL+} = -\Gamma_{nL-}$) $\Gamma_{nR+} = \Gamma_{nR-}$ ($\Gamma_{nR+} = -\Gamma_{nR-}$), $\Gamma_{nL+}\Gamma_{nR+} = \Gamma_{nL-}\Gamma_{nR-}$ is satisfied. Then, $C(\theta)$ in eq.(III.3) becomes zero and $I(\varphi = 0) = I(\varphi = \pi) = 0$ consistent with curve (a) in Fig 2B. For $(\alpha, \beta) = (0, \pi/4)$ or $(\alpha, \beta) = (\pi/4, 0)$, $\Gamma_{nL+}\Gamma_{nR+} = -\Gamma_{nL-}\Gamma_{nR-}$ is satisfied. Then, $A(\theta)$ in eq.(III.3) becomes zero and the resulting $I(\varphi = \pm\pi/2) = 0$ is consistent with curves (b) and (c) in Fig 2B.

Next, we show the α and β dependence of Q for $-\pi/4 \leq \alpha \leq \pi/4$ and $-\pi/4 \leq \beta \leq \pi/4$. It is remarkable that the maximum value of $|Q|$ becomes almost 0.4 and it means the generation of the gigantic diode effect by tuning α and β . Also, by changing (α, β) to $(-\alpha, -\beta)$, $Q = Q(\alpha, \beta)$ satisfies

$$Q(\alpha, \beta) = -Q(-\alpha, -\beta). \quad (\text{III.7})$$

We can show this relation analytically as follows. Since $\Gamma_{nL\pm}$ and $\Gamma_{nR\pm}$ change into $\Gamma_{nL\mp}$ and $\Gamma_{nR\mp}$ by the transformation (α, β) to $(-\alpha, -\beta)$, $\Lambda_{dn}(\theta) = \Lambda_{dn}(\theta, \varphi, \alpha, \beta)$, $\Lambda_{ne} = \Lambda_{ne}(\theta, \alpha, \beta)$, and $\Lambda_{no} = \Lambda_{no}(\theta, \alpha, \beta)$ satisfy

$$\Lambda_{dn}(\theta, \varphi, -\alpha, -\beta) = \Lambda_{dn}(\theta, -\varphi, \alpha, \beta),$$

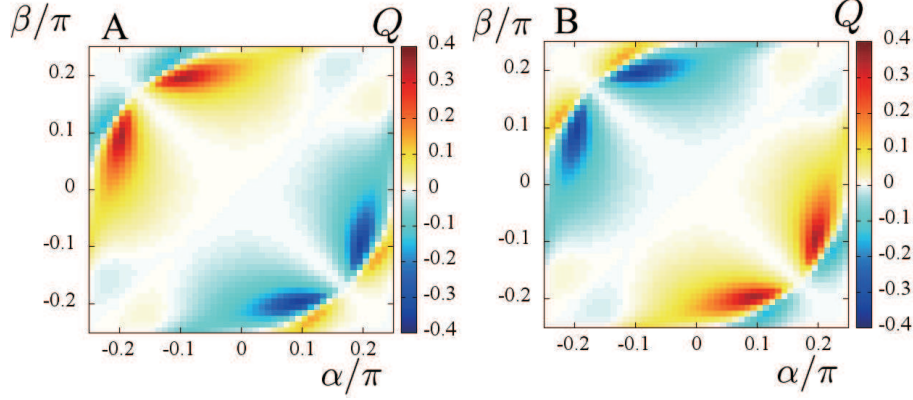


FIG. 3. Q is plotted for various α and β for $T = 0.05T_d$ and $d \mid m_z \mid / v = 1$. (a) $m_z = 0.5\mu$, (b) $m_z = -0.5\mu$.

and

$$\Lambda_{ne}(\theta, -\alpha, -\beta) = \Lambda_{ne}(\theta, \alpha, \beta), \quad \Lambda_{no}(\theta, -\alpha, -\beta) = \Lambda_{no}(\theta, \alpha, \beta)$$

If we write α, β dependence of $I(\varphi)$ explicitly,

$$I(\varphi, \alpha, \beta) = -I(-\varphi, -\alpha, -\beta)$$

is obtained and it leads to eq. (III.7).

It is interesting how nonreciprocal effect depends on the temperature. As shown in Fig. (4), Q is enhanced at low temperature and has a sign change at $T = T_p$ with $T_p \sim 0.78T_d$. As shown in curves (a) and (b) in Fig.4A, the overall sign of Q is reversed with the sign change of m_z .

The corresponding I_c^- and I_c^+ is plotted as curves (a) and (b) for $m_z = 0.5\mu$ in Fig.4B and those for $m_z = -0.5\mu$ in Fig.4C. If we denote m_z dependence of I_\pm explicitly, $I_c^\mp(m_z = 0.5\mu) = -I_x^\pm(m_z = -0.5\mu)$ to be consistent with eq. (III.2). In the inset of Fig.4B, $|I_c^\pm|$ is plotted in the enlarged scale from $0.7T_d < T < T_d$. $I_c^+ = |I_c^-|$ is satisfied for $T = T_p$ when Q becomes zero as shown in Fig. 4B.

To elucidate the exotic CPR specific to nonreciprocal nature of Josephson current, we focus on its Fourier components. In general, Josephson current is decomposed into

$$I(\varphi) = \sum_n [I_n \sin n\varphi + J_n \cos n\varphi] \quad (\text{III.8})$$

For $\alpha = -0.2\pi$ and $\beta = 0.09\pi$, I_1 , I_2 , and J_1 become nonzero values (Figs. 5A and B).

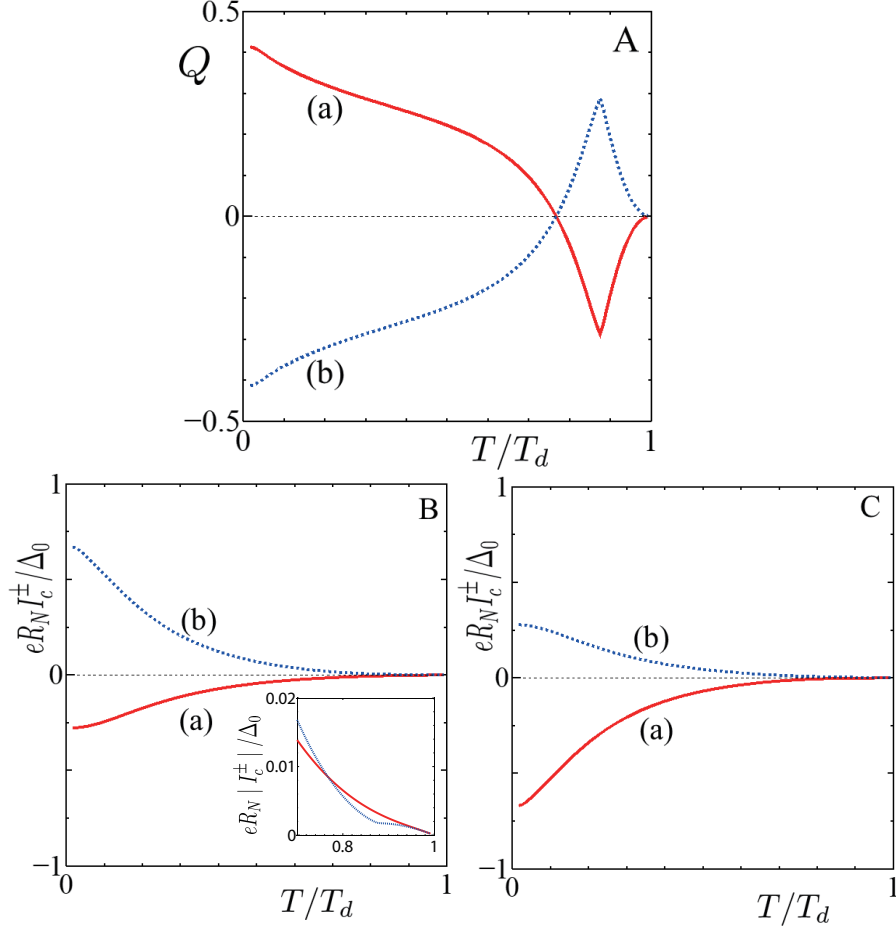


FIG. 4. Temperature dependences of Q , I_c^+ and I_c^- are plotted for $\alpha = -0.2\pi$, $\beta = 0.09\pi$ and $d |m_z| / v = 1$. A: Q for (a) $m_z = 0.5\mu$, (b) $m_z = -0.5\mu$. B: (a) I_c^- and (b) I_c^+ for $m_z = 0.5\mu$. In the inset, $|I_\pm|$ is plotted for $0.7T_d < T < T_d$. C: (a) I_c^- and (b) I_c^+ for $m_z = -0.5\mu$.

By changing m_z to $-m_z$, I_1 and I_2 are invariant and J_1 has the sign change as shown in Figs. 5A and B. As shown in the inset of Fig. 5B, I_1 has the sign change at $T = T_p$. At this temperature, as shown in Fig. 4A, Q becomes zero. We also show I_1 , I_2 , and J_1 for $\alpha = 0$ and $\beta = 0.25\pi$ in Figs. 5C and D. In this case, the resulting Q is zero since the term proportional to $A = A(\theta)$ in eq. (III.3) becomes zero, and the resulting I_1 becomes zero independent of the sign of m_z .

Similar to the case for Figs. 5A and B, I_2 is invariant and J_1 has a sign change by changing m_z to $-m_z$. To summarize, the simultaneous existence of I_1 , I_2 and J_1 is necessary to obtain nonzero Q .

Next, we discuss the energy spectrum of the Andreev bound states since it crucially

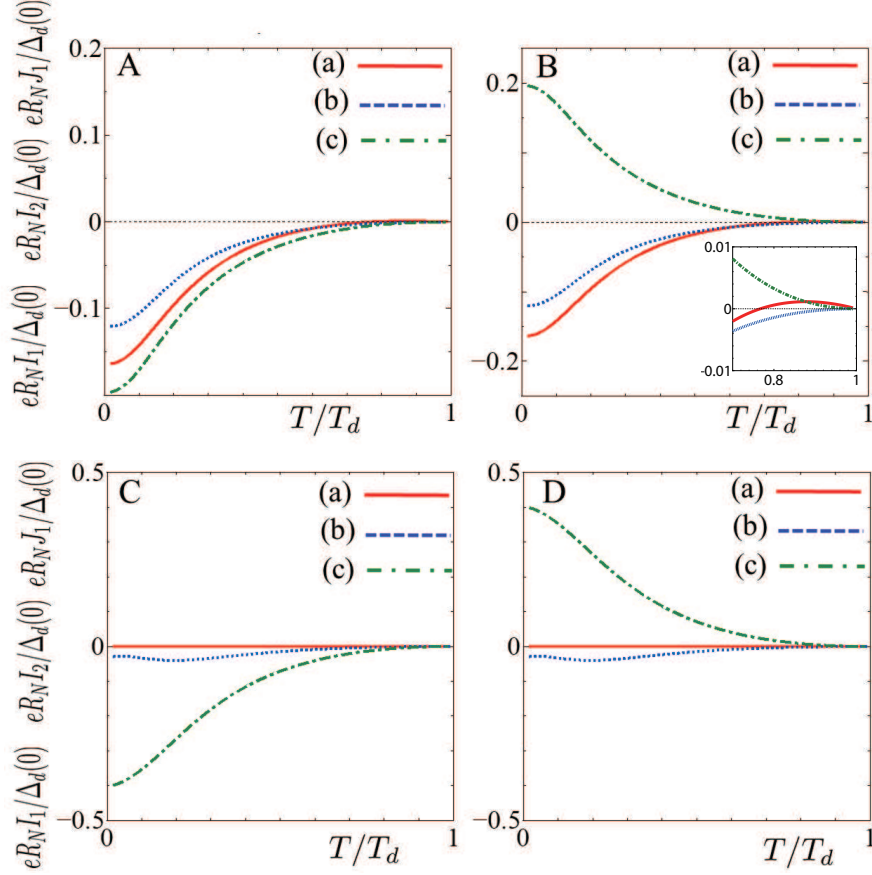


FIG. 5. Temperature dependences of (a) I_1 , (b) I_2 and (c) J_1 are plotted for $d |m_z| / v = 1$. A: $(\alpha, \beta) = (-0.2\pi, 0.09\pi)$ with $m_z = 0.5\mu$, B: $(\alpha, \beta) = (-0.2\pi, 0.09\pi)$ with $m_z = -0.5\mu$, C: $(\alpha, \beta) = (0, 0.25\pi)$ with $m_z = 0.5\mu$, and D: $(\alpha, \beta) = (0, 0.25\pi)$ with $m_z = -0.5\mu$. The enlarged plot for $0.7T_d < T < T_d$ is shown in B as the inset.

determines $I(\varphi)$ [22, 23, 35–37]. Due to the strong spin-momentum locking of the surface states of topological insulator (TI), the Andreev bound states in the present S/F/S junction become Majorana bound states [29, 32, 38–40]. The energy eigenvalues of Majorana bound states (MBS) E_b are found by the zero of $\Lambda_d(E, \theta)$ defined in eq. (II.13) for

$$|E_b| < \min(|\Delta_{L+}|, |\Delta_{L-}|, |\Delta_{R+}|, |\Delta_{R-}|) \quad (\text{III.9})$$

Only for limited cases, we can obtain the energy level of E_b analytically. For $\alpha = \beta = 0$, the energy level of the ABS is expressed by

$$E_b = \pm \sqrt{\sigma_N \cos^2 \frac{\varphi}{2} + (1 - \sigma_N) \sin^2 \frac{\eta}{2}} |\cos 2\theta| \Delta_0 \quad (\text{III.10})$$

with

$$\cos^2 \frac{\eta}{2} = \frac{m_z^2 \cos^2 \theta}{m_z^2 \cos^2 \theta + \mu^2 \sin^2 \theta}, \quad \sin^2 \frac{\eta}{2} = \frac{\mu^2 \sin^2 \theta}{m_z^2 \cos^2 \theta + \mu^2 \sin^2 \theta}$$

to be consistent with the result of s -wave superconductor junction shown in Ref. 32. E_b becomes zero for $\varphi = \pm\pi$ and $\theta = 0$.

On the other hand, for $\alpha = \beta = \pi/4$, E_b becomes

$$E_b = \pm \sqrt{\sigma_N \cos^2 \frac{\varphi}{2} + (1 - \sigma_N) \cos^2 \frac{\eta}{2}} |\sin 2\theta| \Delta_0. \quad (\text{III.11})$$

E_b is zero for $\varphi = \pm\pi$ and $\theta = \pm\pi/2$ or $\varphi = \pm\pi$ and $\theta = 0$. In this case, pair potential also becomes zero and E_b is absorbed into the continuum level. For $\theta = 0$ and $\varphi = \pi$, we can show $E_b = 0$ for wide variety of parameters for $-\pi/4 < \alpha < \pi/4$ and $-\pi/4 < \beta < \pi/4$. In this case, $\Gamma_{L+} = \Gamma_{L-} = \Gamma_L$ and $\Gamma_{R+} = \Gamma_{R-} = \Gamma_R$ are satisfied. Then, $\Lambda_d(E, \theta)$ becomes

$$\Lambda_d(E, \theta = 0) = (1 - \sigma_N) (1 + \Gamma_R^2) (1 + \Gamma_L^2) + \sigma_N (1 + \Gamma_L \Gamma_R)^2 \quad (\text{III.12})$$

Since $\cos(2\alpha)$ and $\cos(2\beta)$ become positive numbers, Γ_R and Γ_L become $-i$ at $E = 0$ and $\Lambda_d(E, \theta) = 0$ at this condition. This means $E_b = 0$ and the ubiquitous presence of Majorana zero mode for various α and β at $\varphi = \pm\pi$ and $\theta = 0$.

In general, it is impossible to solve E_b analytically, and we plot inverse of $\Lambda_d(E, \theta) = \Lambda_d(E, \theta, \varphi)$

$$S(E, \theta, \varphi) = \frac{1}{|\Lambda_d(E, \theta, \varphi)|}. \quad (\text{III.13})$$

The intensity plot of $S(E, \theta, \varphi)$ for fixed φ is shown in Fig. 6. In the actual calculation we replace E for $E + i\delta$ with a small number $\delta = 0.001\Delta_0$ to avoid the divergence, where we have used the value of Δ_0 at zero temperature.

We first show the contour plot of $S(E, \theta, \varphi)$ for fixed value of φ . The blight curve satisfying eq. (III.9) corresponds to the position of E_b . As shown in Fig. 6A, $S(E, \theta, \varphi)$ shows a complicated θ dependence for $\alpha = -0.2\pi$, $\beta = 0.09\pi$ where nonreciprocal effect is prominent as discussed in Figs. 2, 3 and 4. For all cases (A, B and C),

$$S(E, \theta, \varphi) \neq S(E, -\theta, \varphi)$$

and by changing $\varphi = 0.5\pi$ to -0.5π , $S(E, \theta, \varphi)$ shows dramatically different behavior as shown in Fig.6B as compared to that in Fig.6A. For $\varphi = \pi$, $S(E = 0, \theta, \varphi)$ is enhanced

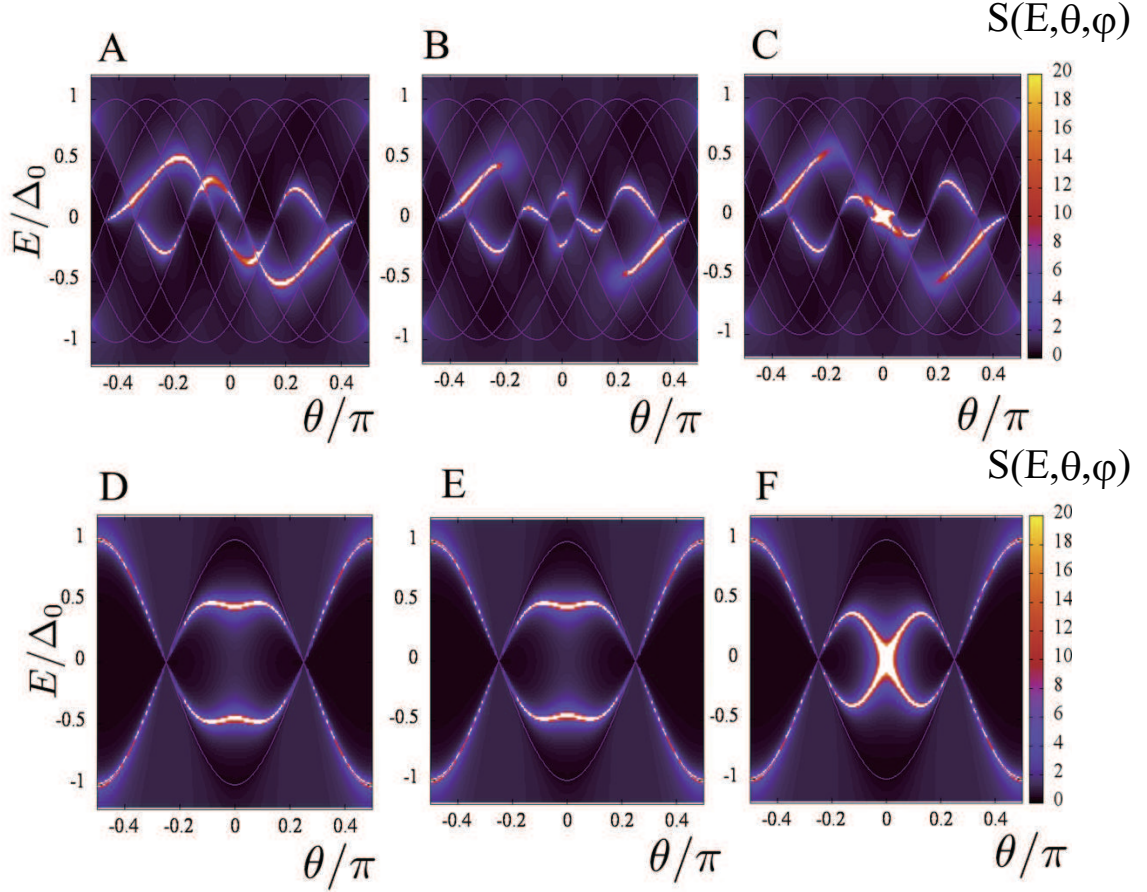


FIG. 6. The intensity plot of $S(E, \theta, \varphi)$ for fixed φ for $d \mid m_z \mid /v = 1$ and $m_z = 0.5\mu$. $(\alpha, \beta) = (-0.2\pi, 0.09\pi)$ for A, B and C. $(\alpha, \beta) = (0, 0.25\pi)$ for D, E and F. A: $\varphi = 0.5\pi$, B: $\varphi = -0.5\pi$, and C $\varphi = \pi$. D: $\varphi = 0.5\pi$, E: $\varphi = -0.5\pi$, and F $\varphi = \pi$. We plot $\pm\Delta_0 \cos[2(\theta \pm \alpha)]$ and $\pm\Delta_0 \cos[2(\theta \pm \beta)]$ as auxiliary lines.

around $\theta = 0$ (Fig.6C) due to the existence of Majorana zero mode at $E = 0$. On the other hand, for $\alpha = \beta = 0$, $S(E, \theta, \varphi)$ shows a symmetric function with θ (Figs. 6D, E and F)

$$S(E, \theta, \varphi) = S(E, -\theta, \varphi), \quad S(E, \theta, \varphi) = S(E, \theta, -\varphi) \quad (\text{III.14})$$

to be consistent with eq. (III.10).

In Fig. 7, we focus on φ dependence of $S(E, \theta, \varphi)$ for fixed θ with $\alpha = -0.2\pi$ and $\beta = 0.09\pi$. By changing θ to $-\theta$, $S(E, \theta, \varphi)$ has a dramatic change. MBS is located for $E > 0$ for $\theta = 0.1\pi$ while it is located for $E < 0$ for $\theta = -0.1\pi$ (Figs. 7A and D). On the other hand, if we change $m_z = 0.5\mu$ to $m_z = -0.5\mu$, MBS is located for $E < 0$ for $\theta = 0.1\pi$ while it is located for $E > 0$ for $\theta = -0.1\pi$ (Figs. 7B and C). Finally, we mention how the

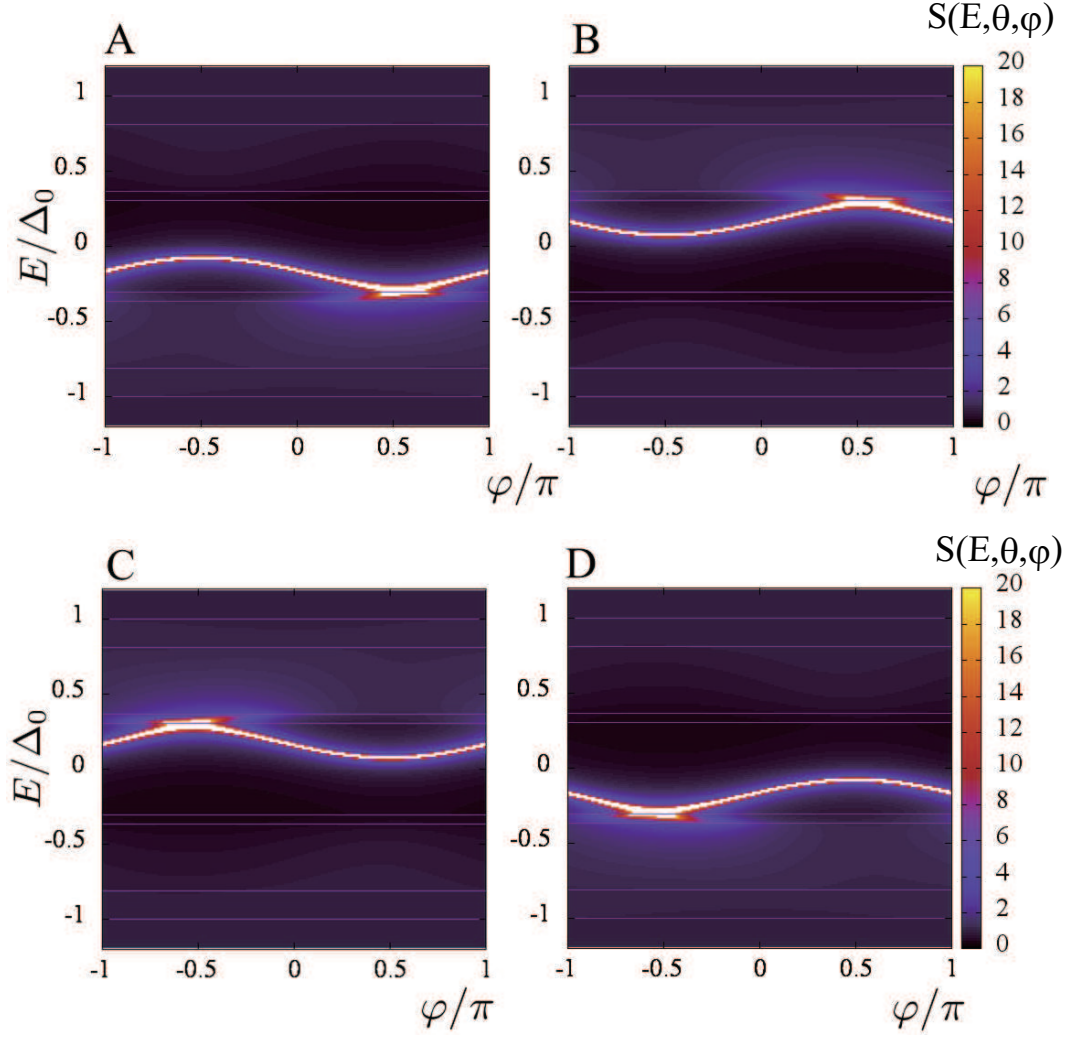


FIG. 7. The intensity plot of $S(E, \theta, \phi)$ for fixed θ for $d |m_z| / v = 1$, $\alpha = -0.2\pi$ and $\beta = 0.09\pi$. A: $\theta = 0.1\pi$ and $m_z = 0.5\mu$, B: $\theta = -0.1\pi$ and $m_z = 0.5\mu$, C: $\theta = 0.1\pi$ and $m_z = -0.5\mu$, and D: $\theta = -0.1\pi$ and $m_z = 0.5\mu$. We plot $\pm\Delta_0 \cos[2(\theta \pm \alpha)]$ and $\pm\Delta_0 \cos[2(\theta \pm \beta)]$ as auxiliary lines.

energy level of E_b changes by the transformation from m_z to $-m_z$. By using the properties of $\Gamma_{R\pm}$, $\Gamma_{L\pm}$, and η , $\Lambda(E, \theta, \phi) = \Lambda(E, \theta, \phi, m_z)$ and $S(E, \theta, \phi) = S(E, \theta, \phi, m_z)$ satisfy

$$\begin{aligned} \Lambda_d(E, -\theta, \phi, -m_z) = & [1 - \sigma_N] [1 + \exp(-i\eta) \Gamma_{R+} \Gamma_{R-}] [1 + \exp(i\eta) \Gamma_{L+} \Gamma_{L-}] \\ & + \sigma_N [1 - \exp(-i\phi) \Gamma_{L+} \Gamma_{R+}] [1 - \exp(i\phi) \Gamma_{L-} \Gamma_{R-}] \end{aligned} \quad (\text{III.15})$$

and

$$\Lambda_d(E, -\theta, -\phi, -m_z) = \Lambda_d(E, \theta, \phi, m_z), \quad S(E, -\theta, -\phi, -m_z) = S(E, \theta, \phi, m_z).$$

We can see these results by comparing Fig.7A (7C) and Fig. 7B (7D).

IV. CONCLUSION

In this paper, we have shown that d -wave superconductor / Ferromagnetic insulator / d -wave superconductor junction on topological insulator can show a very large nonreciprocity of Josephson current. We have found the large magnitude of quality factor Q which characterizes the diode effect by tuning the crystal axis of both left and right d -wave superconductors. The magnitude of Q becomes almost 0.4 at low temperature and its sign is reversed by changing the direction of the magnetization in FI. We have analyzed the Fourier components of Josephson current and found that the simultaneous existence of $\sin \varphi$, $\cos \varphi$ and $\sin 2\varphi$ terms are necessary to obtain nonzero Q . The resulting Q has a strong temperature dependence. These exotic features of Q and current-phase relations stem from the unconventional φ and momentum dependence of Majorana bound states at the interface. These results can serve as a guide to design Josephson diode using Majorana fermion on the surface of TI.

ACKNOWLEDGMENTS

Y.T. was supported by Scientific Research (A) (KAKENHIGrant No. JP20H00131), and Scientific Research (B) (KAKENHIGrants No. JP18H01176 and No. JP20H01857). B.L was supported by National Natural Science Foundation of China (project 11904257) and the Natural Science Foundation of Tianjin (project 20JCQNJC01310).

-
- [1] Y. Tokura and N. Nagaosa, Nat. Commun. **9**, 3740 (2018).
 - [2] G. Rikken, J. Folling, and P. Wyder, Phys. Rev. Lett. **87**, 236602 (2001).
 - [3] V. Krstic, S. Roth, M. Burghard, K. Kern, and G. Rikken, J. Chem. Phys. **117**, 11315 (2002).
 - [4] F. Pop, P. Auban-Senzier, E. Canadell, G. L. J. A. Rikken, and N. Avarvari, Nat, Commun. **5**, 3757 (2014).
 - [5] G. Rikken and P. Wyder, Phys. Rev. Lett. **94**, 016601 (2005).
 - [6] T. Ideue, K. Hamamoto, S. Koshikawa, M. Ezawa, S. Shimizu, Y. Kaneko, Y. Tokura, N. Nagaosa, and Y. Iwasa, Nat. Phys. **13**, 578 (2017).
 - [7] S. Hoshino, R. Wakatsuki, K. Hamamoto, and N. Nagaosa, Phys. Rev. B **98**, 054510 (2018).

- [8] R. Wakatsuki, Y. Saito, S. Hoshino, Y. M. Itahashi, T. Ideue, M. Ezawa, Y. Iwasa, and N. Nagaosa, *Science Advances* **3**, e1602390 (2017).
- [9] F. Qin, W. Shi, T. Ideue, M. Yoshida, A. Zak, R. Tenne, T. Kikitsu, D. Inoue, D. Hashizume, and Y. Iwasa, *Nat. Commun.* **8**, 14465 (2017).
- [10] Y. M. Itahashi, T. Ideue, Y. Saito, S. Shimizu, T. Ouchi, T. Nojima, and Y. Iwasa, *Science Advances* **6**, eaay9120 (2020).
- [11] F. Ando, Y. Miyasaka, T. Li, J. Ishizuka, T. Arakawa, Y. Shiota, T. Moriyama, Y. Yanase, and T. Ono, Observation of superconducting diode effect, *NATURE* **584**, 373+ (2020).
- [12] J. J. He, J. Wu, T. P. Choy, X. Liu, Y. Tanaka, and K. T. Law, *Nat. Commun.* **5**, 3232 (2014).
- [13] A. Daido and Y. Yanase, *Phys. Rev. B* **100**, 174512 (2019).
- [14] N. F. Q. Yuan and L. Fu, *Proc. Nat. Acad. of Sci.* **119**, e2119548119 (2022).
- [15] S. Ilić and F. S. Bergeret, *Phys. Rev. Lett.* **128**, 177001 (2022).
- [16] T. Karabassov, I. V. Bobkova, A. A. Golubov, and A. S. Vasenko, *arXiv:arXiv:2203.15608*.
- [17] R. S. Souto, M. Leijnse, and C. Schrade, *arXiv:arXiv:2205.04469*.
- [18] H. Wu, Y. Wang, Y. Xu, P. K. Sivakumar, C. Pasco, U. Filippozzi, S. S. P. Parkin, Y.-J. Zeng, T. McQueen, and M. N. Ali, The field-free josephson diode in a van der waals heterostructure, *Nature* **604**, 653 (2022).
- [19] K. Misaki and N. Nagaosa, *PHYSICAL REVIEW B* **103**, 245302 (2021).
- [20] C.-R. Hu, *Phys. Rev. Lett.* **72**, 1526 (1994).
- [21] Y. Tanaka and S. Kashiwaya, *Phys. Rev. Lett.* **74**, 3451 (1995).
- [22] S. Kashiwaya and Y. Tanaka, *Rep. Prog. Phys.* **63**, 1641 (2000).
- [23] T. Löfwander, V. S. Shumeiko, and G. Wendin, *Supercond. Sci. Technol.* **14**, R53 (2001).
- [24] S. Yip, *J. Low Temp. Phys.* **91**, 203 (1993).
- [25] Y. Tanaka and S. Kashiwaya, *Phys. Rev. B* **53**, R11957 (1996).
- [26] Y. Tanaka and S. Kashiwaya, *Phys. Rev. B* **56**, 892 (1997).
- [27] Y. S. Barash, H. Burkhardt, and D. Rainer, *Phys. Rev. Lett.* **77**, 4070 (1996).
- [28] G. Testa, E. Sarnelli, A. Monaco, E. Esposito, M. Ejrnaes, D.-J. Kang, S. H. Mennema, E. J. Tarte, and M. G. Blamire, *Phys. Rev. B* **71**, 134520 (2005).
- [29] L. Fu and C. L. Kane, *Phys. Rev. Lett.* **100**, 096407 (2008).
- [30] J. Linder, Y. Tanaka, T. Yokoyama, A. Sudbo, and N. Nagaosa, *Phys. Rev. Lett.* **104**, 067001 (2010).

- [31] B. Lu, K. Yada, A. A. Golubov, and Y. Tanaka, Phys. Rev. B **92**, 100503 (2015).
- [32] Y. Tanaka, T. Yokoyama, and N. Nagaosa, Phys. Rev. Lett. **103**, 107002 (2009).
- [33] A. Furusaki and M. Tsukada, Solid State Commun. **78**, 299 (1991).
- [34] Y. Tanaka and S. Kashiwaya, J. Phys. Soc. Jpn. **69**, 1152 (2000).
- [35] A. Furusaki and M. Tsukada, Phys. Rev. B **43**, 10164 (1991).
- [36] C. W. J. Beenakker and H. van Houten, Phys. Rev. Lett. **66**, 3056 (1991).
- [37] H.-J. Kwon, K. Sengupta, and V. M. Yakovenko, Eur. Phys. J. B **37**, 349 (2004).
- [38] A. R. Akhmerov, J. Nilsson, and C. W. J. Beenakker, Phys. Rev. Lett. **102**, 216404 (2009).
- [39] K. T. Law, P. A. Lee, and T. K. Ng, Phys. Rev. Lett. **103**, 237001 (2009).
- [40] J. Linder, Y. Tanaka, T. Yokoyama, A. Sudbo, and N. Nagaosa, Phys. Rev. Lett. **104**, 067001 (2010).